ARTICLE

THE ANALYST
www.rsc.org/analyst

Functional lipid microstructures immobilized on a gold electrode for voltammetric biosensing of cholera toxin

Quan Cheng,*[a] Shimin Zhu,[b] Jie Song[b] and Na Zhang[a]

[a] *Department of Chemistry, University of California, Riverside, CA 92521, USA*

[b] *Lawrence Berkeley National Laboratory, Materials Sciences, Division, Berkeley, CA 94720, USA*

Received 3rd December 2003, Accepted 16th February 2004
First published as an Advance Article on the web 15th March 2004

Redox functionalized microstructures of diacetylene lipids containing cell surface ligand GM1 have been prepared for the construction of an electrochemical biosensor for cholera toxin from *Vibrio cholerae*. Incorporation of lipid molecules with disulfide functionality into the microstructures allows for firm attachment of the microstructures on a gold surface to form a sensing interface. The observed morphology of the microstructures is platelet, with size around 240 nm as determined by dynamic light scattering and transmission electron microscopy. The electrochemical response stems from electron transfer between the electrode and the redox sites on the microstructures, and the Faradaic current is influenced by the binding events of protein toxins to the ligands displayed on the crystalline surface. Electrochemical characterization indicates that electron transfer of surface ferrocene on the gold electrode is facile. Differential pulse voltammetry was used to measure the current magnitude as a function of toxin concentration, and a working range expanding from 1.0×10^{-8} to 5.0×10^{-7} M was obtained. Bovine serum albumin (BSA) was used as a control agent with which no interference to Faradaic response was found in the same concentration range. Atomic force microscopy (AFM) was used to characterize the morphology and distribution of microstructures on the gold surface. The effectiveness of the design for bypassing surface fouling of proteins in electrochemical detection has been demonstrated, and a binding regulated electron hopping mechanism for the observed electrochemical behavior has been proposed.

Introduction

There is a growing need for new analytical techniques capable of fast, sensitive, and reliable detection of pathogenic agents such as bacterial toxins and microbes. These methods would offer effective tools for use in clinical diagnostics, food safety monitoring, epidemic control, and most recently, counter-terrorism campaigns. Detection of bacterial toxins is of particular importance as many toxins are major determinants of bacterial virulence, and thus responsible for toxic activity and infection even without infestation by the microbes.[1] For instance, cholera toxin (CT), secreted by the bacterium *Vibrio cholerea*, is a known causative agent for diarrhea in humans.[1] In recent years, detection of cholera toxin has drawn considerable research interest largely because (a) there exists a clinical need for developing such a biosensor, and (b) the interaction between CT and its cell surface ligand is well-characterized, making it ideal for testing various detection schemes that target bacterial toxins.[2–6] Cholera toxin binds to cell membrane ligand ganglioside GM1, a glycosphringolipid containing a pentasaccharide headgroup and a ceramide tail. Upon binding, the catalytic domain of CT is inserted into the cell to trigger activation of adenylate cyclase, leading to elevated cAMP levels and eventually, cell lysis.[7] The binding constant of CT to GM1, as recently determined by surface plasmon resonance (SPR) measurement, is in the picomolar range.[8] Several analytical methods have been developed for CT where the recognition is based on either GM1 or CT-specific antibody. Singh and coworkers reported a method of fluoroimmunoassay for detecting CT with ganglioside-bearing liposomes.[9] Ligler and co-workers developed microarray sensors for both direct and "sandwich" immunoassays for CT,[5] and recently expanded it to simultaneous detection of both toxins and bacteria.[10] Swanson and co-workers reported optical CT sensors utilizing fluoroscein and energy-transfer fluorophore labeled GM1.[11] Colorimetric sensors utilizing conjugated polymers (*e.g.*, polydiacetylenes) have been successfully developed by incorporating GM1 into the optically sensitive lipid membranes prepared by forming bilayer liposomes or through Langmuir-Blodgett technique.[12,13]

One important development in CT detection is to fabricate electrochemical (EC) sensors with high sensitivity and low cost. Willner and coworkers reported an EC sensor using QCM and GM1-functionalized liposomes in which high detection sensitivity was achieved.[14] The same group recently reported an ion-selective field-effect transistor sensor coupled with SPR for CT analysis.[15] Another promising method in EC sensing is to explore voltammetric detection of toxins by using chemically functionalized surfaces. The difficulty in voltammetric signaling, however, is that most toxins are non-electroactive. Therefore, a specific interface that links binding events to direct or lateral electron transfer has to be developed. We reported an EC biosensor for *E. coli* enterotoxin using redox microstructures (vesicles) immobilized on a sol gel thin-film electrode.[16,17] Binding of toxins to ligand molecules on the vesicles blocks the electron-hopping path, resulting in decrease of Faradaic current of the redox probes. The membrane-based platform to host biosensory elements used in these studies allows for fast access of target molecules to the sensing interface for detection, and thus provides relatively high detection sensitivity. However, the thin sol gel coating on the electrode was required for immobilization of redox vesicles, the casting of which can be time-consuming and cumbersome.[17]

In this paper, we report an electrochemical biosensor for cholera toxin using redox lipid microstructures attached directly on a gold surface. To ensure the firm attachment of microstructures to the electrode, we take advantage of high affinity between thiol and gold substrate in self-assembled monolayer technique, and incorporate sulfur-containing lipids into the microstructures. Fig. 1 shows the structure of the lipids used in this study. Gly-PDA is an amino acid terminated lipid that form stable microstructures such as liposomes and microcrystalline ribbons,[18,19] and is thus used as the matrix lipid. The redox signal is generated by the ferrocene derivatized lipid, Fc-PDA.[17] Two sulfur-containing compounds, methionine and cysteine-dimethylester, were attached *via* an amide linkage to the diacetylene lipid and used as the "anchor" molecules. For comparison purpose, we also synthesized a double-chained lipid with quaternary amino cation headgroup (Amn-PDA) since this lipid forms stable vesicular structures.[20] Various compositions are

DOI: 10.1039/b315656g

tested to screen out the best formula that forms microstructures with optimal electrochemical response. The microstructure morphology and the distribution of microstructures on the gold surface are investigated because these factors have significant impact on the electrochemical behavior of the sensing interface. Voltammetric characterization (cyclic voltammetry and differential pulse voltammetry) are carried out to study the properties of the modified layer and their sensing characteristics against the targeted toxins and the control agents.

Experimental

Apparatus

Cyclic voltammetry and differential pulse voltammetry were carried out with CV-50W and Epsilon voltammetric analyzers, both from Bioanalytical Systems Inc. (West Lafayette, IN, USA). The electrochemical cell consists of a three-electrode configuration, with a gold disk electrode (1.6 mm in diameter from BAS) as the working electrode, Ag/AgCl in 3 M NaCl as reference and a Pt wire as the auxiliary electrode.

Materials and synthesis

Synthesis of the amino acid derivatized diacetylene lipids is through formation of a *N*-hydroxysuccinimide (NHS)-activated intermediate of the diacetylene lipid, 10,12-pentacosadiynoic acid (GFS Chemicals, Powell, Ohio), followed by amidation with corresponding amino acids. The detailed synthesis of Gly-PDA and Met-PDA is described elsewhere.[18] Fc-PDA[17] and Amn-PDA[20] were prepared by previously reported methods. Monosialoganglioside GM1 was purchased from Matreya (Pleasant Gap, PA, USA) with over 98% purity. Cholera toxin and bovine serum albumin (BSA) were obtained from Sigma. All solutions were prepared in deionized water purified with a Millipore water system.

Cys-PDA 4

Lipid **4** was prepared by direct coupling of NHS-PDA[21] and the commercially available L-cystine dimethyl ester dihydrochloride (Aldrich, Milwaukee, WI) under carefully controlled basic conditions. L-cystine dimethyl ester dihydrochloride (611 mg) was stirred in 5 mL dichloromethane and solublized with addition of triethylamine (494 μL, 2 eq.) at room temperature. NHS-PDA (828 mg, 1 eq.) was dissolved in 15 mL dichloromethane, to which the L-cystine dimethyl ester solution was added dropwise. The reaction was allowed to continue at room temperature for 6–8 h, with periodic addition of a drop of triethylamine. The reaction was monitored by silica gel thin layer chromatography (49:1 chloroform:methanol) *via* the formation of single-chained lipid **4** (R_F = 0.13) and double-chained side product (R_F = 0.75), along with the gradual disappearance of NHS-PDA (R_F = 0.89). To avoid extended exposure to access basic conditions that could cause the undesired β-elimination, the reaction was stopped when roughly 90% of NHS-PDA was consumed. Crude products were concentrated under reduced pressure and subject to silica gel flash chromatography purification using 49:1 chloroform:methanol as an eluting solvent. Spectroscopically pure **4** (624 mg) and double-chained side product (286 mg) were isolated. Only single-chained compound **4** was used in the fabrication of lipid microstructures reported here. Cys-PDA **4**. ^{1}H NMR (500 MHz, $CDCl_3$): δ 6.38 (1H, d, *J* = 7.5 Hz), 4.87 (1H, m), 3.76 (1H, m), 3.74 (3H, s), 3.72 (3H, s), 3.21 (1H, dd, *J* = 14, 5 Hz), 3.16 (1H, dd, *J* = 14.5, 5 Hz), 3.06 (1H, dd, *J* = 13.5, 5 Hz), 2.90 (1H, dd, *J* = 13.5, 7.5 Hz), 2.21 (2H, t, *J* = 7 Hz), 2.20 (4H, t, *J* = 7 Hz), 1.80 (2H, b), 1.60 (2H, m), 1.47 (4H, m), 1.32 (m), 1.22 (m), 0.84 (3H, t, *J* = 7 Hz); ^{13}C NMR (125 MHz, $CDCl_3$): δ 174.08, 172.88, 170.96, 77.55, 77.39, 65.25, 65.18, 53.44, 52.69, 52.35, 51.57, 43.88, 40.67, 36.37, 31.86, 29.59, 29.57, 29.55, 29.43, 29.29, 29.11, 29.10, 29.05, 28.87, 28.81, 28.72, 28.31, 28.26, 25.30, 22.64, 19.16, 19.14, 14.07; HRMS FAB$^+$ (NBA): $C_{33}H_{57}N_2O_5S_2$ [M + H]$^+$, calcd 625.3709, found 625.3696.

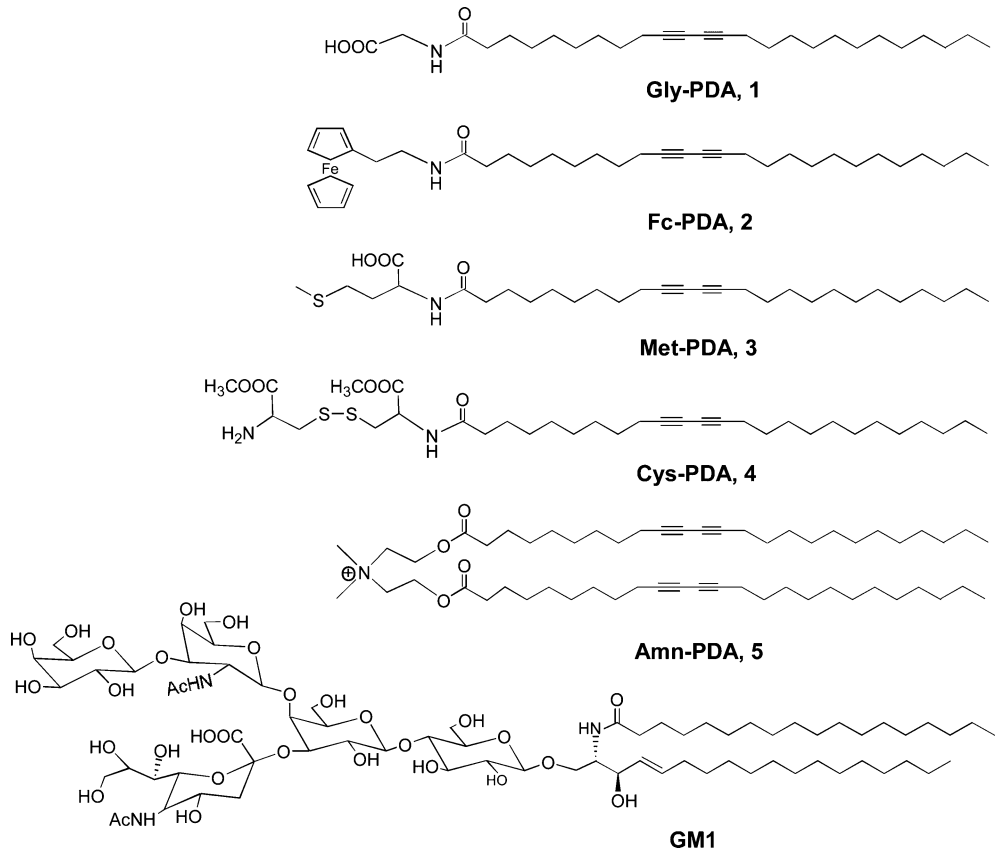

Fig. 1 Structure of the diacetylene lipids and cell surface ligand GM1 used in construction of functional microstructures.

Preparation of microstructures

The microstructures were prepared by probe sonication of related lipids in a buffer solution. Lipids in varied molar ratios were mixed in chloroform and the organic solvent was removed by purging N_2 to form a thin film of lipids in the vial. A buffer solution containing 20 mM HEPES and 0.15 M NaCl at pH 7.5 was added to bring the final lipid concentration to 1 mg mL^{-1}. The solution was then sonicated at low amplitude for 20 min to get a clear solution followed by incubation at 4 °C for 1 h before use.

Characterization of microstructures

A Zeiss transmission electron microscope was used to characterize the microstructures. For better image contrast, negative staining of the samples by uranyl acetate was performed. Size distribution of the microstructures was determined using a Coulter N4 Plus particle analyzer. Atomic force microscopy was performed on a home-built unit. The samples in the AFM experiments were prepared on a gold surface fabricated through vacuum deposition on a silicon wafer substrate.

Electrochemical procedure

The gold disk electrode (1.6 mm in diameter) was pretreated by polishing with 0.1 μm γ-Al_2O_3, followed by a bath sonication and repeated scans between 0.0 V and 1.7 V at a scan rate of 100 mV s^{-1} in 1 M H_2SO_4. After extensive rinsing with DI water and drying at room temperature, an aliquot of 15 μL solution of microstructures was pipetted onto the electrode and allowed for adsorption for 30 min. After rinsing, the electrode was kept in 0.1 M PBS buffer before use.

The effect of toxin binding on the voltammetric response was characterized using a previously published protocol.[18] In short, the microstructure-functionalized electrode was first scanned using differential pulse voltammetry (DPV) from 0.0 to 0.7 V in a 0.1 M PBS buffer solution (pH 7.4), and the anodic peak current was collected as $i_{p,100}$. The electrode was then removed from the solution and rinsed. An aliquot of 15 μL toxin solution was transferred to the electrode surface and allowed for binding with toxin for 5 min. The toxin-bound electrode was returned to the original PBS solution, and the current was measured as $i_{p,s}$. The normalized current response was calculated as $(i_{p,s}/i_{p,100}) \times 100\%$.

Results and discussions

1 Electrochemical characterization of lipid microstructures

We first investigated the effect of lipid composition on formation of microstructures and their electrochemical behavior. Table 1 summarizes some of the lipid compositions we tested and the correspondent redox properties. The screening of microstructure composition was limited to two matrix lipids: Gly-PDA and Amn-PDA, as these two molecules can form stable microstructures.[20,22] Depending on preparation procedure, Gly-PDA in fact can form both vesicles and ribbon-like crystalline microstructures.[22] To ensure a sufficiently large redox response, the molar ratio of the matrix lipid to redox lipid Fc-PDA was fixed at 4:1 while other components including "anchor" lipids varied. The "anchor" lipids used here include Cys-PDA and Met-PDA. The disulfide and thioether groups in these molecules should result in strong attachment of the microstructures on a gold surface. GM1 is a cell surface ligand that is used to recognize the targeted cholera toxin.

Cyclic voltammetry and differential pulse voltammetry were employed to characterize the microstructures adsorbed on the gold surface. Although the amount of Fc-PDA in various samples is virtually the same, the voltammetric response varies significantly (Table 1). Well-defined, nearly symmetric response with reversible electrochemical characteristics ($\Delta Ep < 10$ mV) is denoted as "good" response, while the totally irreversible response is denoted as "poor" one. Most of the microstructures showed fair to good voltammetric response except those of composition #1, 6 and 9 where poor electrochemical behavior was observed. It is interesting to note that microstructures containing GM1 exhibit well-defined voltammetric response, suggesting that in addition to its role as ligand for cholera toxin binding, GM1 may also contribute to the stabilization of lipid microstructures that favors the electron transfer.

2 Stability of voltammetric response

The stability of the voltammetric response for the surface-bound microstructures is of great importance to quantitative analysis of CT. Variation of peak current *versus* time was thus investigated when multiple scans were performed. As indicated in the last column in Table 1, there seems to be no direct correlation between the amount and type of "anchor" lipids and the voltammetric stability. Compositions #4 and #5 showed fair stability as compared to other compositions, and therefore were selected as the compositions for initial characterization.

We first investigated the effect of "anchor" lipids on the electrochemical behavior of the microstructures. Fig. 2 compares the cyclic voltammograms of composition #3 and #5 on a gold electrode in PBS buffer. For composition #5, a symmetric response (curve A) is obtained. The ratio of anodic and cathodic peak current, $i_{p,a}/i_{p,c}$, is close to 1, and the peak separation ΔEp is less than 10 mV, indicating a fast electrochemical process. This is further supported by a relative narrow half-peak width (116 mV). Curve B is the cyclic voltammogram for composition #3 in the same potential window. The peak current decreases and broadens, possibly due to repulsive interactions between the charged species. The peak separation has increased to 34 mV, showing a slight decrease in kinetics. Notably, the formal potential for the ferrocene couple in the 3-phase composition #3 (0.28 V) is more negative than that in a 4-phase composition #5 (0.33 V).

Fig. 3 shows the stability of the voltammetric response for the two systems as a function of time. In this study, differential pulse voltammetry was used for characterization since the DPV method provides better quantitative measurements. From Fig. 3A, the response for composition #5 is very stable. The anodic peak current remains virtually the same for scans over a period of 30 min, with a variation less than 2%. However, current decays rapidly for the composition #3 in a similar experiment (Fig. 3B). The current decreases by about 24% as compared to the initial magnitude in a

Table 1 Composition of the redox-active microstructures and their redox properties on Au

	Composition	Molar ratio	Redox response on Au[a]	Stability of response[a]
1	Gly-PDA:Fc-PDA:Cys-PDA	4:1:0.2	+	+
2	Gly-PDA:Fc-PDA:Met-PDA	4:1:1	+ + +	+ +
3	Gly-PDA:Fc-PDA:GM1	4:1:0.25	+ + +	+
4	Gly-PDA:Fc-PDA:Cys-PDA:GM1	4:1:0.1:0.2	+ + +	+ +
5	Gly-PDA:Fc-PDA:Cys-PDA:GM1	4:1:0.2:0.2	+ + +	+ + +
6	Gly-PDA:Fc-PDA:Met-PDA:Cys-PDA	4:1:1:0.1	+	+
7	Amn-PDA:Fc-PDA	4:1	+ + +	+
8	Amn-PDA:Fc-PDA:Met-PDA	4:1:1	+ +	+
9	Amn-PDA:Fc-PDA:Cys-PDA	4:1:0.5	+	+

[a] The response and response stability is denoted as poor (+), fair (++) and good (+++).

30 min period. The experiments show clearly the importance of having anchor lipids in the system.

It should be pointed out that the morphology of the resulting microstructures shifts with the doping of anchor lipids. The microstructures from the 3-phase composition #3 show a bilayer vesicular morphology, as previously reported.[18] The average size of the vesicles is around 200 nm. Fig. 4 shows the TEM image of microstructures from the composition #5, which differs from #3 by one anchor lipid Cys-PDA. The vesicular structures disappear completely, replaced by small crystalline planar platelets. Using dynamic light scattering method, the size of the planar platelets was measured to be 240 ± 103 nm. The large standard deviation indicates varied dimensions of the microstructures, which is consistent with the TEM results (Fig. 4).

Further optimization experiments show if low content of Cys-PDA lipid was used in the mixture, poor adsorption stability resulted. For instance, when the content of Cys-PDA is reduced to 0.1 relative to Fc-PDA (*e.g.*, composition #4), the redox response decreases slowly though the initial response is satisfactory. When the concentration of Cys-PDA exceeds 0.3 relative to Fc-PDA, the microstructures were found to be unstable, decomposing rapidly when stored in the refrigerator. Microstructures from composition #5, with a median Cys-PDA content, can be kept for about a month at 4 °C before they decay into other structural forms that exhibit much weaker redox response.

3 Voltammetric response on toxin's binding to redox microstructures

The functional microstructures from composition #5 were used for voltammetric detection of bacterial toxin CT. Fig. 5 shows the results by DPV measurements. Curve A in Fig. 5 is the normalized response as a function of CT concentration. The binding time used in the study is 5 min. The redox current decreased with increasing concentrations of the toxin, and a dynamic working range from 1.0×10^{-8} to 5.0×10^{-7} M was obtained. This working range is similar to that of a toxin sensor we developed previously using a sol gel coating on a glassy carbon electrode.[18] The control experiment was carried out with the same concentration of BSA solution (curve B), which gives a relatively flat response, around 97.5% of normalized response. The results indicate that the electrode modified with GM1 doped lipid microstructures can provide selective response to cholera toxin while the control reagent BSA does not generate interference to the toxin detection.

4 Proposed response mechanism

The response mechanism for redox doped microstructures has been investigated in detail before.[18] In the previous work on *E. coli* enterotoxin sensor using a sol gel coating functionalized with redox bilayer vesicles, the electrochemical response was proposed to originate from an electron hopping process that is further assisted by the microcracks existing in the sol gel matrix. The toxin binding to the ligands exposed on the surface of vesicles blocks the electron transport path, resulting in a decrease in Faradaic current. We expect a similar mechanism is responsible for the electrochemical behavior observed for redox doped microstructures in this study. Fig. 6 shows a schematic that illustrates the proposed electron hopping mechanism on microstructures. The ferrocene molecules close to the electrode surface first exchange electrons (oxidation) with the metal, and the oxidation propagates throughout the microstructure *via* a hopping mechanism. The binding of cholera

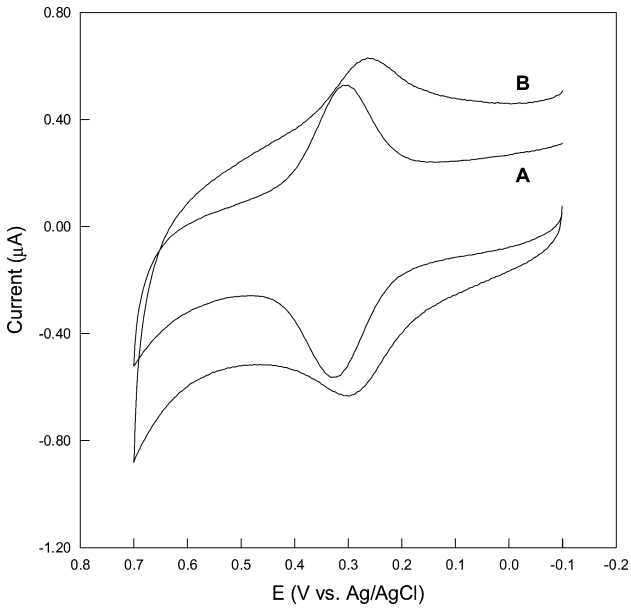

Fig. 2 Cyclic voltammograms of various microstructures adsorbed on a gold electrode. Curve A is the response for microstructures from composition #5 and curve B for composition #3 in 0.1 M, pH 7.4 PBS buffer. The scan rate is 200 mV s^{-1}.

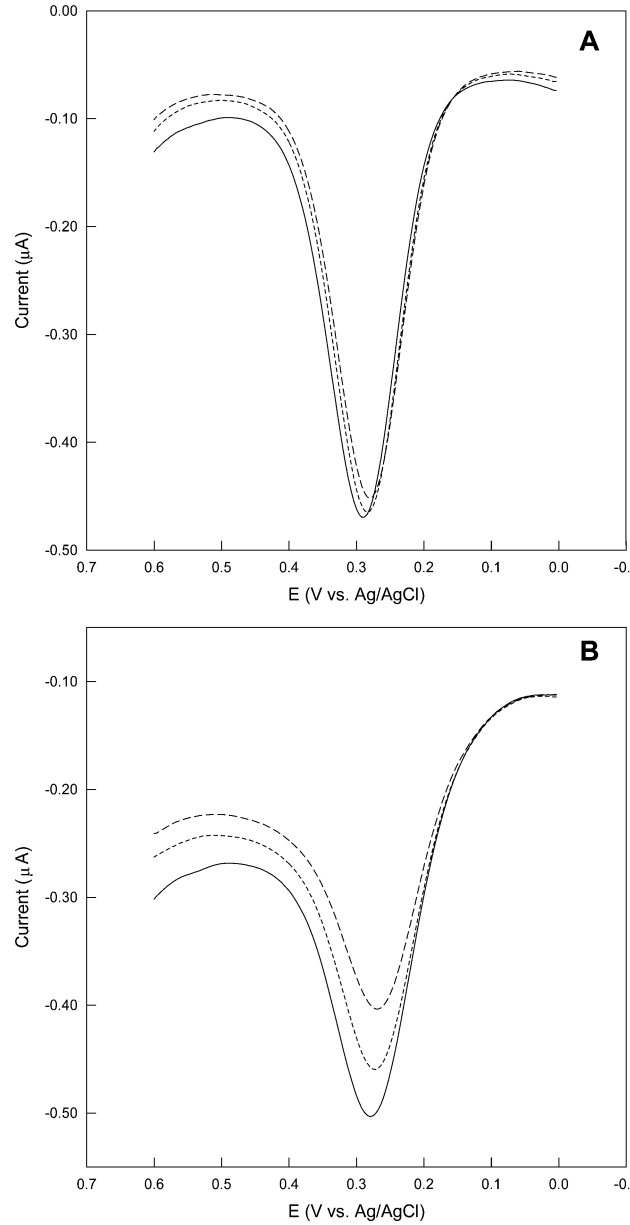

Fig. 3 Differential pulse voltammetric response for microstructures from composition #5 (A) and composition #3 (B) in 0.1 M, pH 7.4 PBS buffer at different times: solid line (—) for $t = 0$ min; dotted line (…) for $t = 15$ min and dash line (– –) for $t = 30$ min. DPV conditions: pulse width is 50 ms, pulse period is 200 ms, and pulse amplitude is 50 mV.

toxin to GM1 on the crystalline surface effectively interferes the electron hopping, either through physical blockage or changing the local solvent environment (*i.e.*, the dielectric constant of the media) for electron transfer. It should be pointed out that total blockage of Faradaic current has not been observed, which is consistent with the model proposed here.

One important parameter for the microstructure-based biosensor is the degree of coverage and the distribution of the microstructures on the surface. Compared to vesicle-based biosensor, the platelet microstructures can be conveniently investigated by atomic force microscopy (AFM). Previously we used AFM to study the molecular packing in lipid-based microstructures, where the atomic resolution makes it possible to identify hexagonal and rectangular packing for flat and twisted regions, respectively.[19] Fig. 7 summarizes the AFM results on the microstructures adsorbed on the gold surface prepared by vacuum deposition on silicon wafers. For a comparison purpose, AFM images of bare gold are also shown. The left column is images obtained in topographic measuring mode (normal force) and the right column is images obtained using friction force. Friction force studies use optical lever technique to measure simultaneous angular deflections of the AFM cantilever due to normal and lateral forces.[23] The friction force measurements are advantageous for features that are not topographically distinct, and can provide some degree of material or chemical sensitivity.[24] This is demonstrated in Fig. 7A where the grain of gold crystalline is clearly visible. Microstructures of the lipid platelets lie flatly on the gold surface with maximal contacts (Fig. 7B and C). The average size of the platelets is comparable with dynamic light scattering and TEM measurements. Profile analysis of the height of microstructures indicates that the platelet has a thickness of roughly 10–12 nm (*ca.* 3 to 4 layers of lipid packing). It is obvious that the surface coverage of microstructures is relatively low, with roughly 15–20% coverage of the total area. It is worth noting that for redox vesicles on sol gel film, high surface coverage was obtained that allows for high degree of electron delocalization, whereas the electron hopping on lipid microstructures will be limited to the surface of individual platelet.

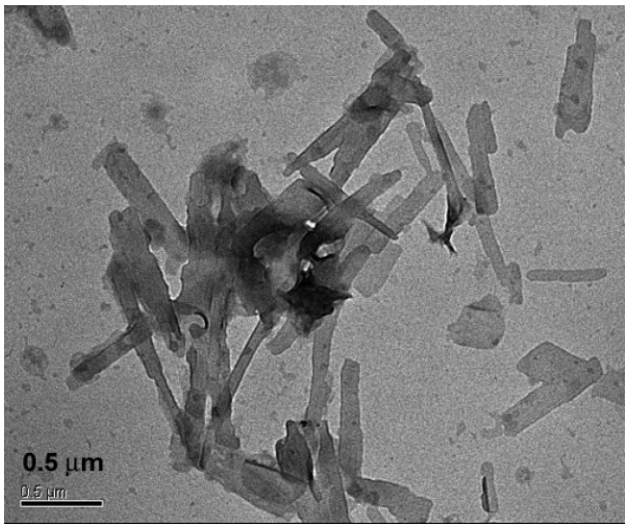

Fig. 4 TEM image of the microstructures formed by composition #5 that shows planar platelet morphology.

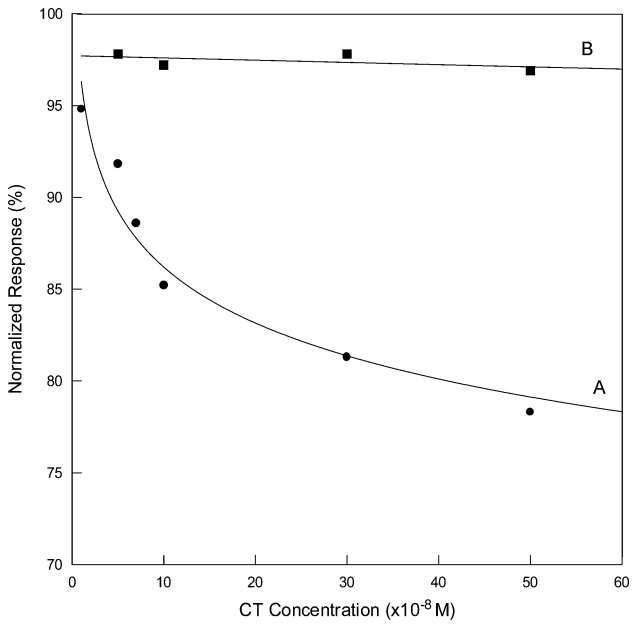

Fig. 5 The normalized response of voltammetric measurements *versus* concentration for bacterial toxin CT (solid circle; curve A) and the control agent BSA (solid square; curve B) obtained by DPV. The potential scans from 0.0 to 0.7 V and the support electrolyte is 0.1 M PBS buffer (pH 7.4). The pulse width is 50 ms, the pulse period 200 ms, and the pulse amplitude 50 mV.

What appears to be puzzling is that a high concentration of BSA seems to have no effect on the voltammetric response of the redox microstructures even with a 15–20% surface coverage (Fig. 5). The surface fouling of the electrode by proteins is a well-known phenomenon. The irreversible nonspecific adsorption of proteins and the subsequent denaturing can effectively block the surface, rendering much slower kinetics and eventually total attenuation of Faradaic current. This does not appear to be the case for the redox microstructure modified electrode (Fig. 5). We believe a different process in mass transport is accountable for the different behavior. For most electrochemical studies involving facile redox process in solution, the response is determined by the diffusion of the redox probes. When protein is present in solution, the adsorption of protein creates an insulating layer on the electrode surface, significantly reducing probe's access and slowing down the electron transfer. For microstructure-modified electrodes, the electron transfer occurs between the electrode and redox centers that are already localized near the surface. The current is carried by the supporting electrolytes that move to balance the electroneutrality interrupted by electron hopping. Nonspecific adsorption

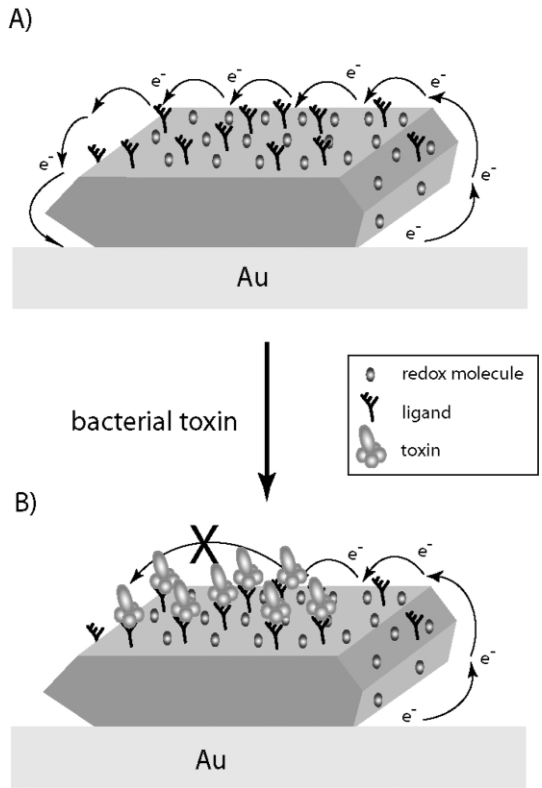

Fig. 6 A schematic of the proposed working mechanism for redox microstructure sensor.

of protein into the bare electrode areas does not affect the voltammetric current, as no electron transfer takes place in those areas. Only the specific binding of targeted proteins onto the ligand sites on the microstructures can block the hopping path, leading to decrease in Faradaic current. In this sense, the redox microstructure-based biosensors presents a unique approach of bypassing surface fouling of proteins in electrochemical detection. The method could find wide applications for detection of target molecules in very complex solutions that contain large concentration of nonspecific proteins.

Conclusions

In this study, we have reported a new biosensor capable of fast, sensitive and amperometric detection of a bacterial toxin, cholera toxin from *Vibrio cholerae*. The sensor was fabricated by immobilization of redox-functionalized microstructures onto a gold surface. The microstructures were formed with diacetylene lipids, which are known to form stable aggregates of varied morphologies. Functionalization of microstructures with cell surface ligand GM1 allowed for specific recognition of target molecule CT, and sulfur-containing anchor lipids ensured firm attachment of microstructures on the gold electrode to realize response stability. We screened a series of matrix lipids and anchor molecules in various compositions for best redox response and response stability. A four-lipid system containing Gly-PDA, Fc-PDA, Cys-PDA and GM1 in a 4:1:0.2:0.2 molar ratio showed desirable redox response and satisfactory stability for making biosensors and was thus used as the working composition. The working range for the sensor was found to extend from 1.0×10^{-8} to 5.0×10^{-7} M, similar to that obtained by a previous vesicle-based biosensor for *E. coli* enterotoxin.[18] BSA was used as a control reagent and showed no interference to toxin sensing in this concentration range.

Compared to the vesicle-based toxin biosensor, the microcrystalline-based sensors have several advantages. Direct adsorption of functional lipid microstructures onto the gold surface offers convenience and ease in preparation. The sol gel coating that was required for hosting vesicle sensing interface in the previous design[18] is no longer needed, eliminating problems stemming from inhomogeneous gel casting. More importantly, this sensor demonstrates that electrochemical detection can be achieved for measuring non-redox proteins through a redox-sensing interface, even on a partially modified electrode surface. Non-specific adsorption of proteins onto the bare gold surface does not affect the electrochemical behavior of the electrode, making it suitable for detecting molecules in a complex medium. Future work will focus on application of the sensors for detection of proteins in biological samples such as blood and other body fluids.

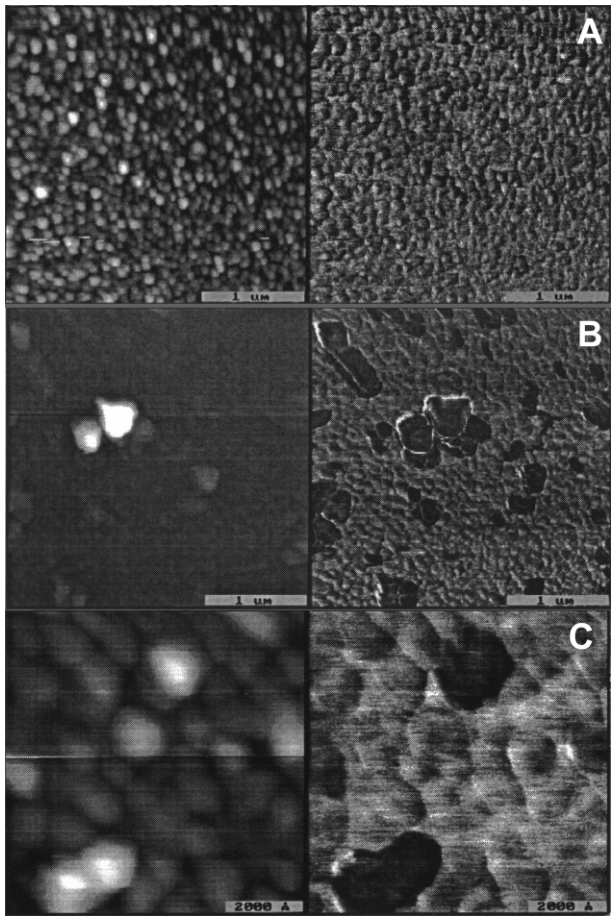

Fig. 7 AFM images obtained by topographic measuring mode (left column) and by friction mode (right column) for microstructures adsorbed on the gold surface prepared by vacuum deposition on silicon wafer. (A) bare gold, (B) microstructures on gold surface and (C) a zoom-in image of microstructures on gold.

Acknowledgement

The authors would like to thank Dr Susanne Kopta of LBNL for the help in the AFM experiments.

References

1 J. E. Alouf and M. W. Palmer, in *The Comprehensive Sourcebook of Bacterial Protein Toxins*, ed. J. E. Alouf and J. H. Freer, Academic Press, London, 2nd edn., 1999.
2 C. R. Taitt, G. P. Anderson, B. M. Lingerfelt, M. J. Feldstein and F. S. Ligler, *Anal. Chem.*, 2002, **74**, 6114.
3 M. Zayats, O. A. Raitman, V. I. Chegel, A. B. Kharitonov and I. Willner, *Anal. Chem.*, 2002, **74**, 4763.
4 G. Puu, *Anal. Chem.*, 2001, **73**, 72.
5 C. A. Rowe-Taitt, J. J. Cras, C. H. Patterson, J. P. Golden and F. S. Ligler, *Anal. Biochem.*, 2000, **281**, 123.
6 M. A. Cooper, A. Hansson, S. Lofas and D. H. Williams, *Anal. Biochem.*, 2000, **277**, 196.
7 *Guidebook to Protein Toxins and Their Use in Cell Biology*, ed. R. Rappuoli and C. Montecucco, Oxford University Press, Oxford, 1997.
8 G. M. Kuziemko, M. Stroh and R. C. Stevens, *Biochemistry*, 1996, **35**, 6375.
9 A. K. Singh, S. H. Harrison and J. S. Schoeniger, *Anal. Chem.*, 2000, **72**, 6019.
10 J. B. Delehanty and F. S. Ligler, *Anal. Chem.*, 2002, **74**, 5681.
11 X. D. Song, J. Nolan and B. I. Swanson, *J. Am. Chem. Soc.*, 1998, **120**, 4873.
12 D. Charych, Q. Cheng, A. Reichert, G. Kuziemko, M. Stroh, J. O. Nagy, W. Spevak and R. C. Stevens, *Chem. Biol.*, 1996, **3**, 113.
13 J. J. Pan and D. Charych, *Langmuir*, 1997, **13**, 1365.
14 L. Alfonta, I. Willner, D. J. Throckmorton and A. K. Singh, *Anal. Chem.*, 2001, **73**, 5287.
15 M. Zayats, O. A. Raitman, V. I. Chegel, A. B. Kharitonov and I. Willner, *Anal. Chem.*, 2002, **74**, 4763.
16 Q. Cheng, T. Peng and R. C. Stevens, *J. Am. Chem. Soc.*, 1999, **121**, 6767.
17 T. Z. Peng, Q. Cheng and R. C. Stevens, *Anal. Chem.*, 2000, **72**, 1611.
18 Q. Cheng, M. Yamamoto and R. C. Stevens, *Langmuir.*, 2000, **16**, 5333.
19 J. Song, Q. Cheng, S. Kopta and R. C. Stevens, *J. Am. Chem. Soc.*, 2001, **123**, 3205.
20 D. A. Frankel and D. F. Obrien, *J. Am. Chem. Soc.*, 1994, **116**, 10057.
21 W. Spevak, PhD Thesis, University of California at Berkeley, 1993.
22 Q. Cheng and R. C. Stevens, *Langmuir.*, 1998, **14**, 1974.
23 E. Barrena, S. Kopta, D. F. Ogletree, D. H. Charych and M. Salmeron, *Phys. Rev. Lett.*, 1999, **82**, 2880.
24 S. Kopta and M. Salmeron, *J. Chem. Phys.*, 2000, **113**, 8249.